

## Enhancing the Accuracy of Computed Tomography Measurements using Data Filtering

Alessandro Stolfi<sup>a</sup>, Maarja-Helena Kallasse<sup>b</sup>, Lorenzo Carli<sup>b</sup>, Leonardo De Chiffre<sup>a</sup>

<sup>a</sup>Technical University of Denmark, Produktionstorvet Building 425 Room 2092800 Kgs. Lyngby Denmark,

email: [alesto@mek.dtu.dk](mailto:alesto@mek.dtu.dk), [ldch@mek.dtu.dk](mailto:ldch@mek.dtu.dk)

<sup>b</sup>Novo Nordisk A/S, Hillerød, 3400, Denmark

email: [mjnk@novonordisk.com](mailto:mjnk@novonordisk.com)

email: [lzcl@novonordisk.com](mailto:lzcl@novonordisk.com)

### Abstract

This paper describes the impact of data filtering on CT capability to inspect assemblies. The investigation was carried out using an industrial multi-material assembly provided by Novo Nordisk A/S. The assembly comprises two parts made of polyoxymethylene (POM) and of an alloy comprising polycarbonate (PC) and acrylonitrile butadiene styrene (ABS), respectively. 3D median filters with different window sizes were taken in account as influence factors, while a variety of dimensional and geometrical tolerances were used as evaluation parameters. All measurands were calibrated using a tactile CMM with uncertainty below 7  $\mu\text{m}$ .

**Keywords:** Computed tomography, dimensional metrology, multi-material measurements, INTERAQCT Marie Curie, data filtering, polymers.

### 1 Introduction

Computed Tomography (CT) represents a profound change in dimensional metrology. CT allows the inner and the outer geometry of an object to be measured without the need of external access or destructive testing [1-3]. CT provides a favourable information-to-measurement-time ratio making it possible to perform a large variety of dimensional inspections by using a data set only. These are just a few of the significant advantages with respect to coordinate measuring machines (CMMs) that are heading increasingly towards the establishment of CT in manufacturing industries dealing with free form and soft parts as well as assemblies. Despite the promising industrial adoption, a lot remains to be done on both the hardware and software side to enhance accuracy and precision of CT measurements. Data filtering may represent a great support tool enhancing the CT measurement accuracy minimising the unwanted signal affecting surface determination and feature fitting. This study evaluates features of 3D median filtering with respect to two variables such as the application stage of filtering within the CT measurement workflow and the kernel size. A multi-material item, including a mix of measurands was selected to explore filtering on a broader front.

### 2 Test workpiece and its calibration

The Workpiece is an assembly component from a commercial insulin injection device from Novo Nordisk A/S (Figure ). The inner component is made of polyoxymethylene (POM). The outer component is made out a mixture of polycarbonate (PC) and acrylonitrile butadiene styrene (ABS). Both are produced using injection molding. Three measurands were selected on the outer part, as shown in a section view in Figure 1b. D1 represents the inner of the smallest cylindrical feature measured at  $z - 3$  mm from the datum B. R1 is roundness of D1. L2 represents the distance between the datum B and a plane on the bottom of the largest cylinder. Likewise, three measurands were selected on the outer part, as shown in a section view in Figure 1c. D3 represents the inner diameter of the smallest cylindrical feature measured at  $z - 5$  mm above the datum A, while R3 represents the roundness of D3. L4 is the distance between the datum B and a plane on the bottom flange. The similarity of measurands was chosen to adequately compare the effect of filtering on both components. Reference measurements were performed using a tactile CMM equipped with a probe with a diameter of 1.5 mm and 0.8 mm for the outer and inner component, respectively. A number of points ranging from 16 to 20 were probed and subsequently fitted using a least square routine. Measurement uncertainties below 7  $\mu\text{m}$  were obtained for both components.

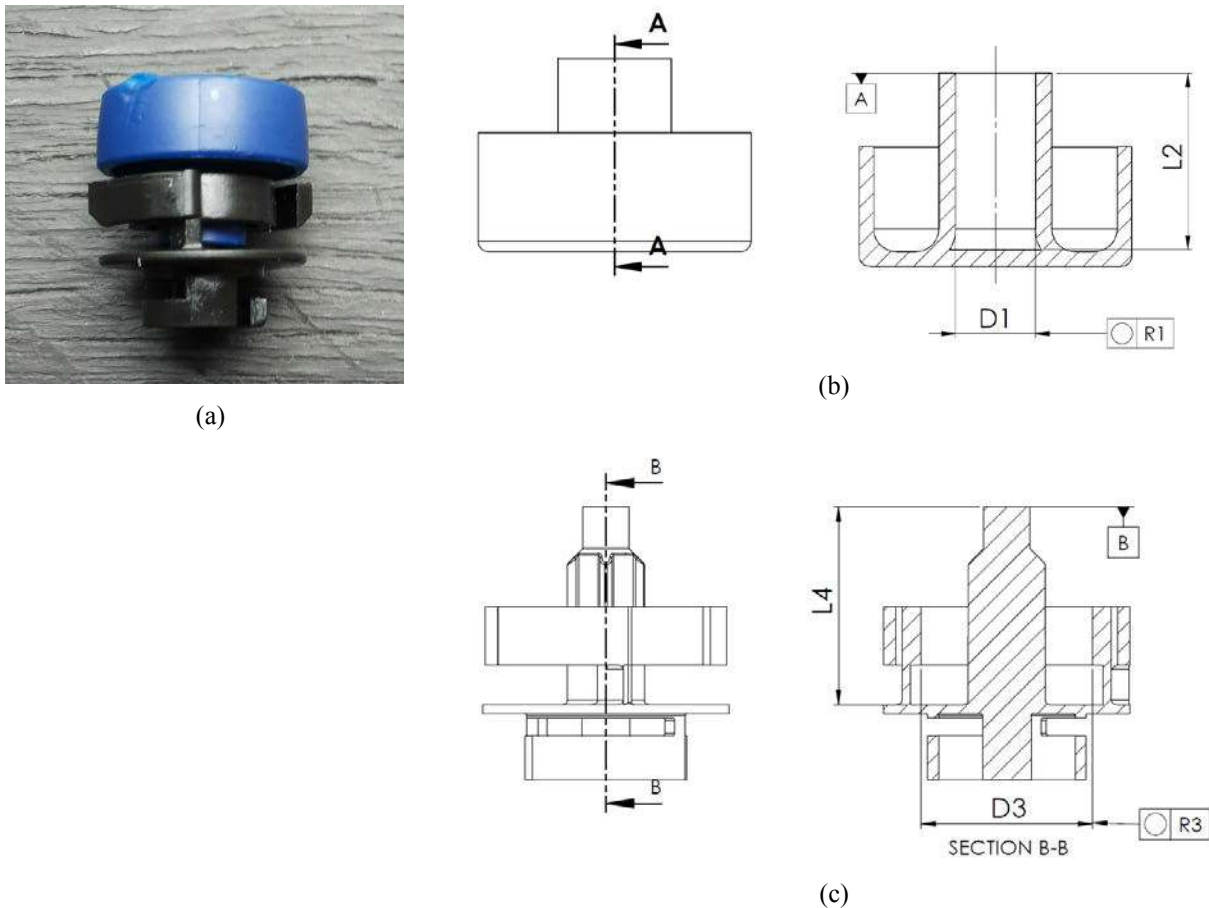


Figure 1: (a) two-part component of an insulin pen and 2D definition of measurands for (b) outer and (c) inner component.

### 3 Experimental plan

Experimental test plan is schematically shown in figure 2. After scanning and reconstructing the stack of x-ray projections, the CT volume model was elaborated using three different workflows: two 3D filtered workflows and one unfiltered workflow, which was only used as a reference throughout the elaborations. The filtered workflows were performed similarly, the only exception being the stage in which the filter was applied, namely before performing surface determination (hereafter “B-SD”) or after the latter (hereafter “A-SD”). Two 3D median filters, characterized by two symmetrical kernels of 3 (hereafter “Small kernel”) and 5 (hereafter “Big kernel”) voxels were investigated because they provide a good noise removal and image segmentation enhancement. Moreover, 3D filters are definitely ease of use compared to 2D filtering requiring software and routines to be performed. The data sets were analysed using VG Studio Max 2.2.6. The surface determination was based on a local adaptive thresholding method (with a search distance of 5 voxels) in which the starting point was selected per data set independently of the other ones. This is necessary to record any change in the histogram of grey values. CMM and CT alignment and evaluations were performed alike, despite having modified the number of points to take full advantage of high density information featuring a CT measurement. All primitive features were least-squares fitted using 500 points (step width of 0.050 mm and search distance of 0.1 mm). The evaluations of geometrical measurands were conducted taking into account the whole distribution of fitted points. The reason for that was not to introduce additional filtering during the evaluations.

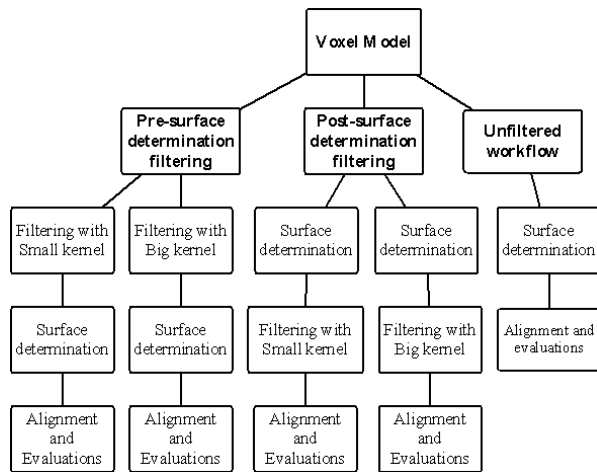


Figure 2 Schematic representation of the experimental test plan.

Parameter	Unit	Value	Parameter	Unit	Value
X-ray tube voltage	KV	100	Magnification		7
X-ray tube current	$\mu\text{A}$	270	No. of projections		1500
Voxel size	$\mu\text{m}$	40	Integration time	ms	1500
Spot size	$\mu\text{m}$	23	No. of images for projection		1

Table 1 Overview of the scanning parameters used.

#### 4 Measuring setup for tactile and CT measurements

A Nikon XT H 225 CT systems was used for the investigation and set according to table 1. The workpiece was scanned 3 times, placed within a low-absorption fixture. A fast shading correction together with a limited number of projections with no averaging were used to have a noise level being acceptable for the purpose of the investigation. The cabinet temperature was logged, found to be  $23 \pm 0.5$  °C, and assumed to correspond to the workpiece one due to the acclimation of a few hours before scanning. The reconstruction was performed on the CT Pro software package provided by Nikon Metrology, while the evaluations were conducted on the voxel-based data sets using VG Studio MAX 2.2.6 inspection software. During the reconstruction a beam hardening correction, based on 2nd order function was applied. The data sets were reconstructed as 32-bit floating point numbers rather than 16-bit integers to have their grey value distributions always comparable at a cost of larger data sets. Since the CT used is not a metrology-designed system, voxel size and temperature must be corrected. The voxel size correction was conducted using a ball-plate [4], as reference artefact, that was scanned twice (at the beginning and the end of three CT scans) in order to also consider the X-ray source drift, as the system ran for approximately 8 hours, including shading correction. The mean scaling factor value was found to be 0.9988, and taken directly into account rescaling the volume in VG studio Max. The correction was based on a few of 300 centre-to-centre distances available in the artefact due to the high magnification used. The correction of thermal deformation was carried out on Solidworks, using an isotropic model to simulate the workpiece, and subsequently taken into account for the dimensional measurands only. Additionally, the temperature did not affect the dimensional stability of workpiece, as negligible deformation in the contact zone between the components took place. The uncertainty assessment was based on the PUMA method (ISO 14253-2) [5], as described in equation 1.

$$U_D^{\text{cal}} = k * \sqrt{u_{\text{cal}}^2 + u_p^2 + u_t^2} \quad (1)$$

where  $k$  is the coverage factor, having a level of confidence of approximately 95 %;  $u_{\text{cal}}$  is standard uncertainty establishing traceability using CMM measurements at  $\sigma$ -confidence level;  $u_p$  is standard uncertainty describing the measurement procedure for each measurand, calculated as  $u_p = s$  is standard deviation from the reproduced measurements,  $u_t$  is temperature-related standard uncertainty calculated for a deviation of  $\pm 0.5$  °C and using a coefficient of linear expansion for both components. No uncertainty contribution associated with the alignment was taken into account because an accurate alignment procedure, based on a best fit, followed by fine-tune alignment was used. Measurement uncertainties are reported per workflow and kernel size in table 2. Measurement uncertainties for length measurement are the greatest ones because the higher sensitivity to surface outliers and to datum system. Repeatability better of  $2 \mu\text{m}$  was registered for majority the measurands due to the robust measurands used, to the efficacy of systematic error corrections performed but also to the absence of repositioning of the item during scanning. It can be observed in the table that the uncertainties for both components lie within the same range. This can be explained by the absence of beam hardening that usually characterizes the scanning of polymer parts.

Component	Measurand	Unfiltered	A-SD (small kernel)	A-SD (Big kernel)	B-SD (small kernel)	B-SD (Big kernel)
Outer	D1	12	12	12	12	12
	R1	12	13	12	12	12
	L2	21	20	20	20	20
Inner	D3	14	14	14	15	15
	R3	12	12	13	13	12
	L4	21	20	19	20	20

Table 2 Expanded uncertainties at 95% confidence level for the measurands of the two parts. Values in  $\mu\text{m}$ .

Component	Measurand	Unfiltered	A-SD (small kernel)	A-SD (Big kernel)	B-SD (small kernel)	B-SD (Big kernel)
Outer	D1	0.55	0.42	0.40	0.50	0.56
	R1	0.80	0.66	0.66	0.58	0.53
	L2	0.15	0.15	0.19	0.35	0.36
Inner	D3	0.55	0.42	0.42	0.50	0.52
	R3	0.83	0.66	0.66	0.58	0.55
	L4	0.25	0.25	0.24	0.40	0.50

Table 3 En values for the measurands of the two parts.

## 5 Results and discussion

Results are presented in table 3 using the En criterion which considers deviations for reference quantities and measurement uncertainties simultaneously [6]. In this case, being measurement uncertainties rather constant (see table 2), En values represent deviations. The table shows that generally filtering decreases En values for both components and their measurands. The reduction of En values does not appear to be constant but varies as workflow and kernel size changes. A-SD workflow yielded better En values up to 22% for dimensional measurements independently of kernel size, while B-SD outperformed for geometrical measurements with a reduction of En of approximately of 28%. These results obtained emphasize the substantial difference between the workflows. In the A-SD, filtering is applied on a constrained data set and therefore it can just remove small structures on the surface similarly to a morphological operator such as closing and opening. Filtering within B-SD instead operates on a non-constrained data set and consequently produces a strong flattening by expanding of the data set, as shown in figure 4. Such an expansion resulted in deviations up to 7  $\mu\text{m}$  for Big kernel with respect to the unfiltered data sets. This effect appeared not to be similar for any surface but changes with the noise level characterizing surfaces.

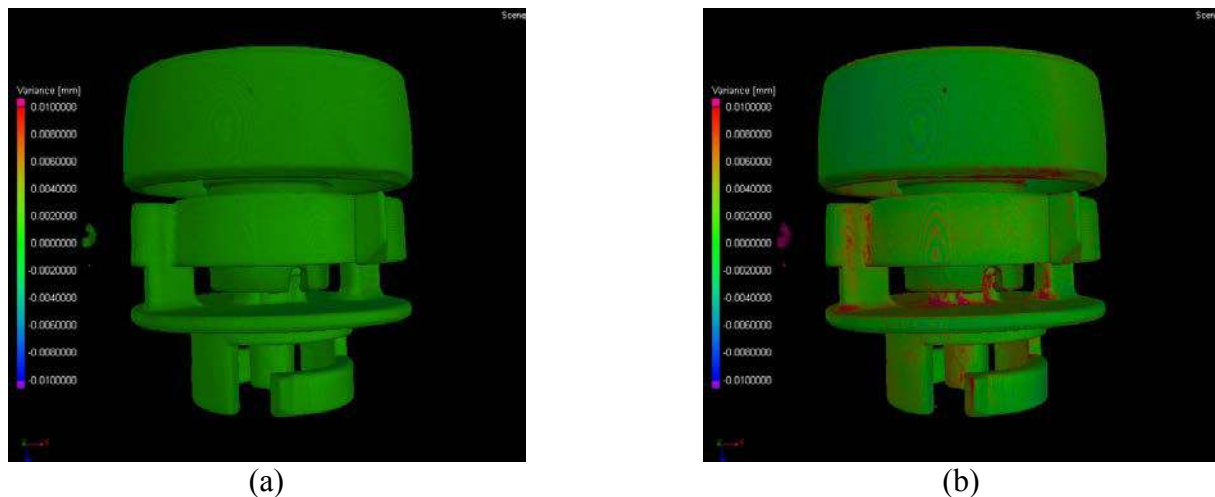


Figure 4 Colour deviation maps showing dimensional differences with respect to the unfiltered volume for (a) A-SD and (b) B-SD workflow, which were filtered using Small kernel.

In A-SD, the two kernel provided results were in very good agreement for diameter and roundness measurements as well as for length measurements. Larger differences were observed for B-SD due to the mentioned expansion of the data sets. Moreover, the two kernels modified asymmetrically the histogram of the residual of fitted points by mainly removing peaks. Negligible differences were noted with respect to the computation time between the workflows in processing the same kernel. Substantial differences were recorded for the computation time. Big kernel took 6 times longer than Small kernel to be completed. Image analysis showed that both workflows yielded a similar reduction of the noise of about 30 % with respect to the unfiltered

workflow. Such a value was quantified using several x-ray slices taken in the XY plane of the CT coordinate system by mean of Fiji imaging analysis software. Imperceptible differences in the shape and extension of the distributions of grey values were observed with respect to the unfiltered one. This was also confirmed by the constancy of the optimal starting point value during surface determination throughout the tests. Furthermore, it was observed that increasing the filtering kernel improves the shape of the edge and the plateau, too (see figure 5). Despite the mentioned results, the differences between the two workflows were not sufficient to reject the null hypothesis of pair t-tests [7] performed for each kernel and for each measurand. The same conclusion was obtained for the kernel sizes. It may be concluded that inverting the filtering stage within the CT workflow or changing the kernel size has no significant effect on the accuracy.

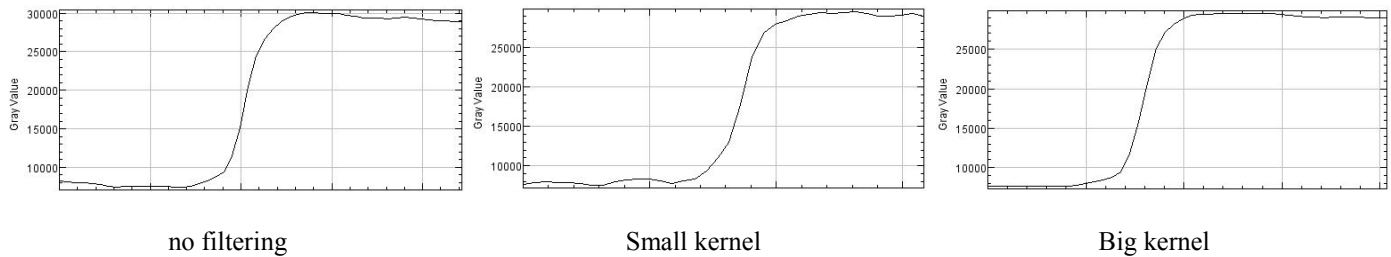


Figure 5 Profile across the edge before and after filtering the data set. Increasing filtering reduces the oscillating signal and makes edges sharper.

## 6 Conclusions

This study evaluates features of 3D median filtering with respect to two variables such as the application stage of filtering within the CT measurement workflow and the kernel size. The following conclusions can be provided:

- The uncertainties of the CT measurements were found to vary between 12 and 20  $\mu\text{m}$  depending on the measurands, and a repeatability better of 2  $\mu\text{m}$  was quantified for all the measurands. Both components showed similar uncertainties and bias that support the absence of beam hardening.
- Filtering decreases  $E_n$  values for both components and their measurands. The accuracy enhancement does not appear to be constant but varies as workflow and kernel size changes. A-SD workflow yielded better  $E_n$  values up to 22% for dimensional measurements regardless of kernel size, while B-SD outperformed for geometrical measurements with a reduction of  $E_n$  of approximately of 28%. A mean noise reduction of approximately 30% was observed similarly for the filtered workflow compared to the unfiltered one.
- The two kernel within the A-SD workflow provided results were in very good agreement for diameter and roundness measurements as well as for length measurements. Slightly larger differences were observed for B-SD due to the allowed expansion of the data sets. Moreover, the two kernels modified asymmetrically the histogram of the residual of fitted points by mainly removing peaks.

## Acknowledgements

The research leading to these results has received funding from the People Programme (Marie Curie Actions) of the European Union's Seventh Framework Programme (FP7/2007-2013) under REA grant agreement no. 607817 INTERAQCT. The authors would like to acknowledge Jakob Rasmussen in connection with the CMM measurements.

## References

- [1] J.-P. Kruth, M. Bartscher, S. Carmignato, R. Schmitt, L. De Chiffre, A. Weckenmann, Computed tomography for dimensional metrology, *CIRP Ann. Manuf. Technol.* 60, 821–842 (2011).
- [2] L. De Chiffre, S. Carmignato, J.-P. Kruth, R. Schmitt, A. Weckenmann, Industrial applications of computed tomography. *CIRP Annals - Manufacturing Technology*, 63(2), 655-677 (2014).
- [3] M. Bartscher, U. Hilpert, J. Goebels, G. Weidemann, Enhancement and proof of accuracy of industrial computed tomography (CT) measurements, *CIRP Ann. Manuf. Technol.* 56, 495–498 (2007).
- [4] P. Müller, J. Hiller, A. Cantatore, G. Tosello, L. De De Chiffre, New reference object for metrological performance testing of industrial CT systems, *Proceedings of the 12th International Conference of the European Society for Precision Engineering and Nanotechnology (euspen) 1(2012) pp. 72-75, ISBN13 978-0-9566790-0-0.*
- [5] ISO 14253-2: 2011 – Geometrical product specifications (GPS) – Inspection by measurement of workpieces and measuring

equipment – Part 2: Guidance for the estimation of uncertainty in GPS measurement, in calibration of measuring equipment and in product verification.

[6] ISO/IEC-17043. Conformity assessment, General requirements for proficiency testing. 2010.

[7] Johnson, R. A. Probability and statistics for engineers. Miller & Freund's, Seventh Edition, 2005. ISBN 0-13-143745-3.